Applied Catalysis B: Environmental 148–149 (2014) 466–472

Contents lists available at ScienceDirect

Applied Catalysis B: Environmental

journal homepage: www.elsevier.com/locate/apcatb

Iridium(0) nanoparticles dispersed in zeolite framework: A highly active and long-lived green nanocatalyst for the hydrogenation of neat aromatics at room temperature

Yalcın Tonbul[a], Mehmet Zahmakiran[b], Saim Özkar[c,*]

[a] On the leave of absence from Ziya Gökalp Faculty of Education, Dicle University, 21280 Diyarbakır, Turkey
[b] Department of Chemistry, Yüzüncü Yıl University, 65080 Van, Turkey
[c] Department of Chemistry, Middle East Technical University, 06800 Ankara, Turkey

ARTICLE INFO

Article history:
Received 18 July 2013
Received in revised form
12 November 2013
Accepted 13 November 2013
Available online 21 November 2013

Keywords:
Iridium
Nanocatalyst
Zeolite
Hydrogenation
Aromatics

ABSTRACT

The complete hydrogenation of aromatic molecules is one of the key transformation employed in the synthetic and petroleum chemistry. Described herein is a new catalytic nanomaterial for the hydrogenation of neat aromatics under mild conditions. A novel nanocatalyst, consisting of iridium(0) nanoparticles stabilized by zeolite with FAU framework could reproducibly been prepared from the reduction of iridium(III)-exchanged zeolite in an aqueous sodium borohydride solution at room temperature and characterized by ICP-MS, P-XRD, HRTEM, XPS, N_2-Ads.-Des., and $P(C_6H_{11})_3$ poisoning. The results reveal the formation of iridium(0) nanoparticles of 5.8 ± 2.1 nm size dispersed on the external surface along with iridium(0) nanolclusters in cavities of zeolite-Y whereby the host matrix remains intact. The resulting iridium(0) nanoparticles were employed as heterogeneous catalyst in the hydrogenation of various aromatic substrates (benzene, toluene, *o*-xylene and mesitylene) in the solvent-free systems at room temperature and 3 bar *initial* H_2 pressure. They are highly active catalyst in the hydrogenation of neat aromatics, such as they can completely hydrogenate benzene to cyclohexane with an *initial* turnover frequency value of TOF = 3215 h^{-1}. Moreover, they show high durability against to leaching and sintering throughout the catalytic runs, which make them reusable catalyst. More importantly, testing the catalytic lifetime of our iridium(0) nanoparticles showed that they provide previously unprecedented total turnover number of TTO = 197,000 over 92 h before deactivation in the hydrogenation of benzene at room temperature and 3 bar *initial* H_2 pressure.

1. Introduction

The complete hydrogenation of aromatic molecules is one of the central reactions for the fine chemicals and intermediates in the petroleum, chemical and pharmaceutical industries [1,2]. For instance, in the petrochemical industry, many of the compounds found in crude oil are of little use since they contain C=C unsaturated bonds; they must be first transformed to their saturated counterparts before commercial use such as gasoline [3]. In the fine chemical and active pharmaceutical ingredient industries, the hydrogenation reaction is often an important step in producing the target products [4]. Most studies regarding the hydrogenation of aromatic compounds have used benzene as the model molecule, and various homogeneous and heterogeneous catalysts have been thoroughly employed in this catalytic transformation [5]. Indeed, benzene is difficult to hydrogenate when compared to olefins because of the resonance stabilization resulting from the strong π-conjugation in the aromatic ring [6]. Thus, hydrogenation reaction conditions often require high temperatures >373 K, initial H_2 pressures >30 atm, and proper organic solvent-systems, leading to generation of by products and requiring product separation procedures. In the literature only a few reports exist on catalyst systems that can perform the complete hydrogenation of benzene under mild conditions (i.e., < 373 K and initial H_2 pressures < 30 atm) and under solvent-free conditions with notable hydrogenation rates (see Table 1 *vide supra*) [7–19].

As seen from the inspection of reports cited in Table 1 (*vide supra*) the majority of these catalysts are suffering from low activity. Therefore, the development of simply prepared, highly active and durable catalytic materials that can hydrogenate neat aromatics under mild conditions still remains a thorny challenge in this research field. Recent reports have already shown that Ru [13–15], Ir [8,17,20] and Rh [18] nanoparticles confined in solid materials can act as highly active hydrogenation catalyst. These

* Corresponding author. Fax: +90 312 210 3200.
E-mail address: sozkar@metu.edu.tr (S. Özkar).

0926-3373/$ – see front matter © 2013 Elsevier B.V. All rights reserved.
http://dx.doi.org/10.1016/j.apcatb.2013.11.017

Table 1
Catalyst systems that can hydrogenate neat benzene to cyclohexane under mild conditions.

Entry	Catalyst	T (K)	P H_2(bar)	TOF [33] (h^{-1})	Reference
1	Rh NPs	298	1.0	48	[7]
2	$[(Cp^*)Zr(CH_3)_3]@Al_2O_3$	298	1.0	2880	[10]
3	Ir NPs	298	1.0	91	[11]
4	Ru NPs@SBA-15	293	3.0	804	[12]
5	Ru NPs@zeolite	295	3.0	1040	[13]
6	Rh@CNT*	298	10.0	1038	[14]
7	Ru@nanozeolite	298	3.0	5430	[15]
8	Ru@HAp*	298	3.0	610	[16]
9	Ir NPs/$[Ir(COD)Cl]_2$@zeolite	295	3.0	1250/47	[17]
10	Rh@HAp	298	3.0	1770	[18]
11	Ru–Ni/C	293	3.0	7905	[19]
12	Ir NPs@zeolite	298	3.0	3190	This study

[a] CNT and HAp stand for carbon nanotube and hydroxyapatite, respectively.

results encouraged us to focus on the development of new supported metal nanoparticles catalyst for this important catalytic transformation. Herein, we report the preparation and characterization of new iridium nanocatalyst, iridium(0) nanoparticles stabilized by zeolite of FAU framework, hereafter referred to as IrNPs@FAU, plus their notable catalytic performance in terms of the activity, selectivity, reusability and lifetime in the hydrogenation of neat aromatics at 298 K with a 3 bar initial H_2 pressure. IrNPs@FAU can be reproducibly prepared from our previously established simple two steps procedure [21,22] comprising of the ion-exchange of Ir^{3+} ions with extra framework Na^+ ions of zeolite followed by their reduction within the zeolite framework by sodium borohydride ($NaBH_4$) in aqueous solution at room temperature. The resultant IrNPs@FAU were characterized by using a combination of advanced analytical techniques including inductively coupled plasma mass spectroscopy (ICP-MS), powder-X-ray diffraction (P-XRD), transmission electron microscopy (TEM), high-resolution-TEM (HRTEM), X-ray photoelectron spectroscopy (XPS), nitrogen-adsorption-desorption (N_2-Ads.-Des.) analyses and $P(C_6H_{11})_3$ poisoning experiments, which reveal that the formation of highly crystalline well-dispersed iridium(0) nanoparticles of 5.8 ± 2.1 nm on the external surface as well as iridium(0) nanoclusters in the cavities of zeolite by keeping the host framework intact.

The resulting IrNPs@FAU were found to be highly active and selective catalyst in the hydrogenation of aromatics in the solvent free systems at room temperature. They provide an *initial* turnover frequency value of TOF = 3215 h^{-1} in the hydrogenation of neat benzene as a model reaction at 298 K and under 3 bar initial H_2 pressure with the complete reduction of benzene to cyclohexane. Moreover, they exhibit high durability throughout their catalytic use in the hydrogenation reaction against agglomeration and leaching. This significant property makes them a reusable catalyst in the hydrogenation of aromatics such that they retain >50% of their *initial* activity even at the fifth catalytic run in the hydrogenation of neat benzene. More importantly, they have a previously unprecedented catalytic lifetime in the hydrogenation of neat benzene by providing a total turnover number of TTO = 197,000 over 92 h before deactivation under the identical conditions given above. Additionally, IrNPs@FAU catalyst system fulfills the majority of the "Green Chemistry" [23] requirements which impose neat/solventless systems whenever possible.

2. Experimental

2.1. Materials

Iridium(III) chloride trihydrate ($IrCl_3{\cdot}3H_2O$), sodium borohydride ($NaBH_4$, 98%), benzene (99%), toluene (99%), *d*-chloroform ($CDCl_3$) and cyclohexane (99%) were purchased from Aldrich. Cyclohexene (99%), mesitylene (98%), and *o*-xylene (98%) were purchased from Fluka. Sodium zeolite-Y (Si/Al = 2.5) was purchased from Zeolyst and slurried with 0.1 M NaCl to remove sodium defect sites, washed until free of chloride and calcined in dry oxygen at 773 K for 12 h before to use. All catalyst reaction solutions were prepared in oxygen free atmosphere (Labconco, drybox). Benzene, toluene, *o*-xylene and mesitylene were distilled over sodium under argon and stored in the drybox. Deionized water was distilled by water purification system (Milli-Q System). All glassware and Teflon coated magnetic stir bars were cleaned with acetone, followed by copious rinsing with distilled water before drying in an oven at 423 K.

2.2. Characterization

The chemical composition of IrNPs@FAU was determined by inductively coupled plasma mass spectroscopy (ICP-MS; Varian-Vista). Powder X-ray diffraction (P-XRD) patterns were acquired on a MAC Science MXP 3TZ diffractometer using Cu-Kα radiation (wavelength 1.5406 Å, 40 kV, 55 mA). Transmission electron microscopy (TEM) was performed on a JEM-2010F microscope (JEOL) operating at 200 kV. XPS analysis performed on a Physical Electronics 5800 spectrometer equipped with a hemispherical analyzer and using monochromatic Al-Kα radiation (1486.6 eV, the X-ray tube working at 15 kV, 350 W and pass energy of 23.5 keV). NMR spectra were recorded on a Bruker Avance DPX 400 (400.1 MHz for 1H) spectra were obtained in $CDCl_3$ in 5 mm o.d. Optima NMR tubes at room temperature and were referenced to the residual solvent impurity. The nitrogen adsorption-desorption experiments were carried out at 77 K using a NOVA 3000 series instrument (Quantachrome Instruments). The sample was outgassed under vacuum at 573 K for 3 h before the adsorption of nitrogen.

2.3. Preparation of iridium(0) nanoparticles stabilized by zeolite framework (IrNPs@FAU)

IrNPs@FAU were synthesized by following a two-step procedure; (i) in the first step, Ir^{3+} ions were introduced into the zeolite by ion-exchange of 1000 mg zeolite in 100 mL aqueous solution of 100 mg $IrCl_3.3H_2O$ (0.29 mmol) for 72 h at room temperature. The sample was then filtered by suction filtration using Whatman-1 filter paper and the remnant was dried in vacuum, (ii) next, the solid remnant was added into $NaBH_4$ solution (100 mL, 264 mM) at room temperature. Ir^{3+} ions were reduced and the iridium(0) nanoparticles were formed; the reduction was considered to be complete when no more hydrogen evolution was observed. The resulting IrNPs@FAU sample was isolated by suction filtration followed by

washing three times with 100 mL of deionized water, and dried under vacuum (10^{-3} Torr) at 353 K, then transferred into the drybox (O_2 < 5 ppm, H_2O < 1 ppm).

2.4. General procedure for IrNPs@FAU catalyzed hydrogenation of aromatic substrates

Hydrogenation reactions were performed using hydrogenation apparatus; a Fischer–Porter pressure bottle modified by Swagelock TFE-sealed quick-connects and connected to a H_2 line and an Omega PX-302 pressure transducer interfaced through an Omega D1131 digital transmitter to a computer using the RS-232 module. The progress of individual hydrogenation reactions was followed by monitoring the loss of H_2 pressure on Lab View 8.0 program.

A similar procedure as described elsewhere [15,16] was followed here; in a drybox the catalyst was weighed into 40 mm × 20 mm borosilicate culture tube containing 5/16 in × 5/8 in Teflon coated magnetic stir bar then the substrate was transferred into this tube via gas-tight syringe. The culture tube was then sealed inside of the Fischer–Porter pressure bottle and Fischer–Porter bottle brought outside of the drybox and placed inside a constant temperature circulating water bath. Next, the hydrogenation line was evacuated for at least 1 h, to remove any trace of oxygen and water present and then the line was refilled with purified hydrogen. The Fischer–Porter bottle was then attached to the hydrogenation line *via* its TFE-sealed Swagelock Quick-Connects and the bottle was purged 10 times (15 s per purge). A timer was started and the pressure in the F–P bottle was then set a constant 3 bar of H_2. The reaction was monitored on PC via RS-232 module and using Lab View 8.0 program. Reaction rates were calculated from the rate of hydrogen pressure loss as determined by the slope of the linear portion of the H_2 uptake curve.

2.5. Testing the isolability and reusability of IrNPs@FAU in the hydrogenation of neat benzene

After the first run of the hydrogenation of 1.0 mL benzene (11.24 mmol), catalyzed by 87 mg IrNPs@FAU (with an iridium loading of 0.34% wt) at 298 K and 3 bar of initial H_2 and > 700 rpm stirring speed the FP bottle was disconnected from the line, taken into the drybox, opened and the content of culture tube was transferred into a Schlenk tube, resealed and connected to the vacuum line. After the evaporation of reaction solution in vacuum the dried sample of IrNPs@FAU was transferred into the glove box. The dried sample of IrNPs@FAU was weighed and used again in the next run of hydrogenation of 1.0 mL of fresh benzene (11.24 mmol) by following the same protocol as described in the previous section. The same procedure was repeated up to 5th cycle. The results were expressed as a percentage of retained initial activity of IrNPs@FAU versus catalytic runs in the hydrogenation of neat benzene.

2.6. Determination of catalytic lifetime of IrNPs@FAU in the hydrogenation of neat benzene

The catalytic lifetime of IrNPs@FAU in the hydrogenation of neat benzene was determined by measuring the total turnover number (TTO), which was started with 87 mg IrNPs@FAU (with an iridium loading of 0.34% wt) that dispersed in 4.0 mL benzene, and then performed in the same way as described in the previous sections. When the complete hydrogenation of benzene is achieved (judged by total H_2 consumption and ^1H NMR) more benzene was added into the solution and the reaction was continued in this way until no hydrogen uptake was observed.

2.7. The leaching test of IrNPs@FAU in the hydrogenation of neat benzene

After the first run of the hydrogenation of 1.0 mL benzene (11.24 mmol), catalyzed by 87 mg IrNPs@FAU (with an iridium loading of 0.34% wt) at 298 K and 3 bar of initial H_2 and > 700 rpm stirring speed, the FP bottle was disconnected from the line, taken into the drybox, opened and a small aliquot from the suspension was taken for ICP-MS analysis, then the rest of the suspension in the culture tube was filtered. The filtrate was transferred into a new culture tube with 0.5 mL fresh benzene. The culture tube was placed into the FP bottle. The hydrogenation of benzene was performed in the same way as described previously.

2.8. Poisoning test of IrNPs@FAU in the hydrogenation of neat benzene

In a three sets of experiments the hydrogenation of 1.0 mL benzene (11.24 mmol), catalyzed by 87 mg IrNPs@FAU (with an iridium loading of 0.34% wt) at identical conditions described above were performed in the presence of 0.05, 0.10 and 0.15 equiv of $P(C_6H_{11})_3$. The relative rates (initial activity in the presence of poison over the one in the absence of poison) were determined for each experiment and given as relative rate vs equiv of $P(C_6H_{11})_3$ plot.

3. Results and discussion

3.1. Preparation and characterization of iridium(0) nanoparticles dispersed in zeolite matrix

IrNPs@FAU with different wt % of iridium loadings were prepared by following the procedure previously described [21,22] that comprises of the ion-exchange of Ir^{3+} with the extra framework Na^+ cations of zeolite, followed by their reduction with sodium borohydride in aqueous solution all at room temperature. It is noteworthy that that the sodium cation site distribution in the zeolite is essentially restored upon reduction [24,25]. The cation sites left by Ir^{3+} ions upon reduction are reoccupied by sodium cations coming from sodium borohydride. Hence, the host framework remains intact as shown also by powder XRD. Fig. 1 shows the powder-X-ray diffraction (P-XRD) patterns of zeolite-Y, Ir^{3+}-exchanged zeolite-Y and IrNPs@FAU samples. The comparison of the patterns given in Fig. 1 shows that there is no noticeable change in both the intensities and positions of the Bragg peaks, indicating that neither the crystallinity nor the lattice of zeolite framework is disturbed by the procedure used for the preparation of IrNPs@FAU.That no peaks are observable for iridium in the P-XRD pattern is due to low concentration of iridum in the sample (0.34 wt.% Ir) as determined by ICP.

The morphology and composition IrNPs@FAU were investigated by TEM, HRTEM, and ICP-MS analyses. The transmission electron microscopy (TEM) image of IrNPs@FAU is given in Fig. 2(a), which shows the presence of well-dispersed iridium(0) nanoparticles on the external surface of zeolite-Y. The mean particle size of iridium nanoparticles was found to be 5.8 ± 2.1 nm (Fig. 2(a) inset) from the TEM image given in Fig. 2(a), whereby 170 non-touching particles were counted. These iridium nanoparticles appear to be stable and do not agglomerate to the bulk metal. In addition, HRTEM image of the IrNPs@FAU given in Fig. 2(c) is indicative of the highly crystalline feature of the resulting iridium nanoparticles, it clearly shows an interplanar spacing of ~0.23 nm, attributable to the {1 1 1} plane of face centered cubic (fcc) Ir [26].

The oxidation state of iridium in the resulting IrNPs@FAU was analyzed by X-ray photoelectron spectroscopy (XPS). The high resolution Ir 4f spectrum of IrNPs@FAU sample (Fig. 3) gives two prominent peaks centered at 63.0 and 66.0 eV, readily assigned to Ir(0) $4f_{7/2}$ and Ir(0) $4f_{5/2}$, respectively [27]. The shifts observed

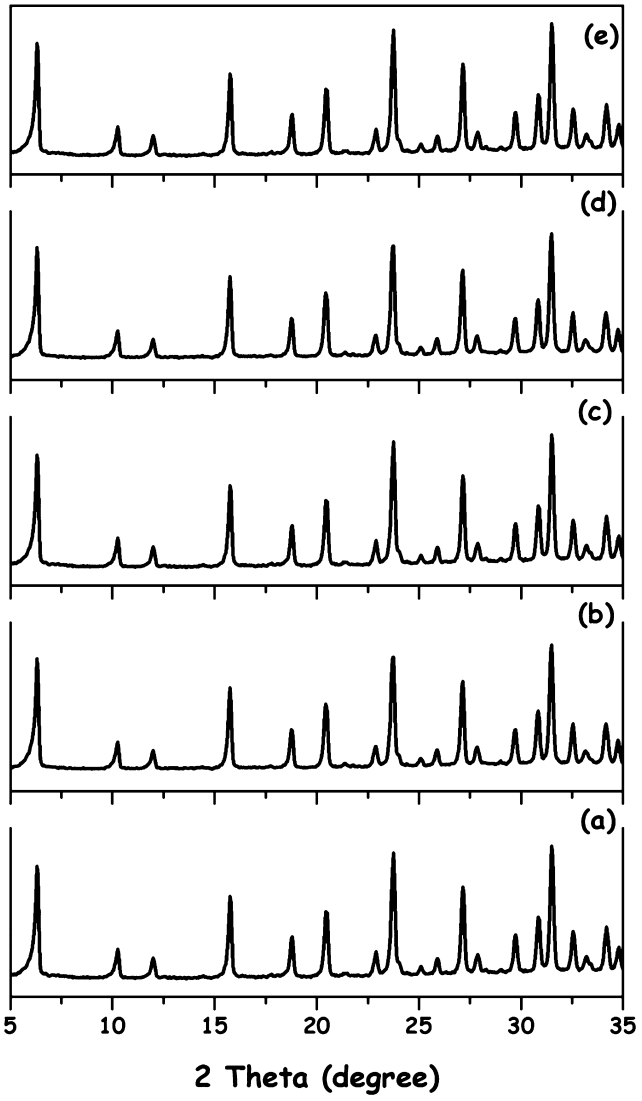

Fig. 1. Powder X-ray diffraction (P-XRD) patterns of (a) zeolite-Y, (b) Ir(III)-exhchanged zeolite-Y, (c) IrNPs@FAU, (d) IrNPs@FAU isolated from the 5th catalytic run, (e) IrNPs@FAU isolated from the catalytic lifetime experiment in the range of $2\theta = 5.0–37.5^{\circ}$.

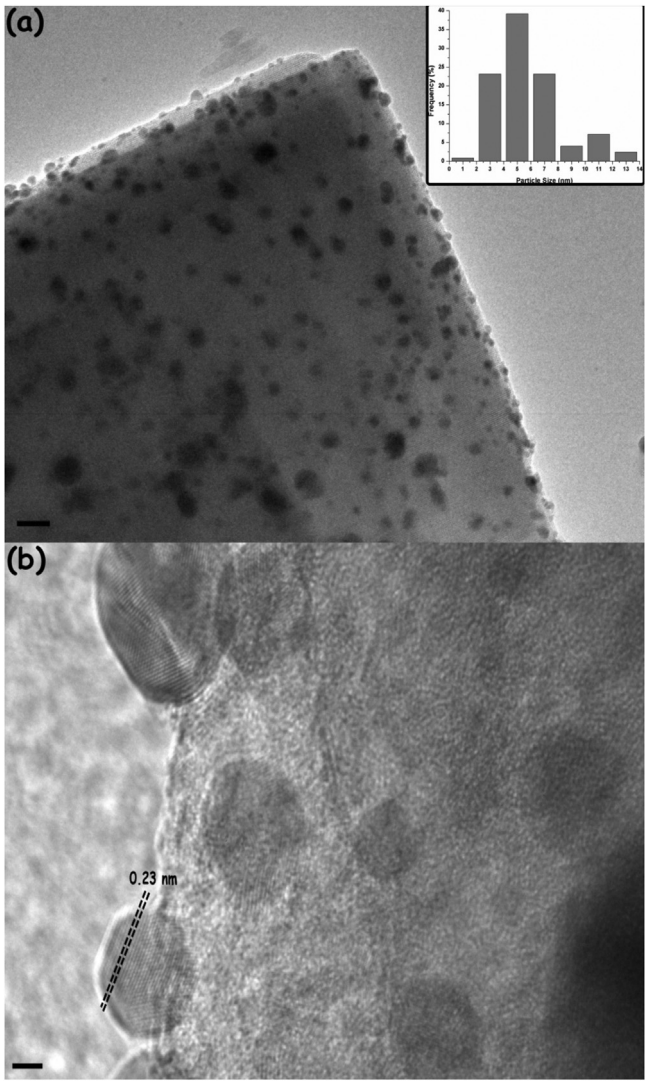

Fig. 2. (a) Transmission electron microscopy (TEM) image of IrNPs@FAU and the corresponding size histogram of IrNPs@FAU, (b) high resolution TEM (HRTEM) image of IrNPs@FAU with an iridium loading of 0.34 wt % scale bars represent (a) 10 nm and (b) 1 nm.

(ΔE_b = 1.2-1.5 eV) in the binding energies of Ir NPs towards higher energy values with respect to metallic iridium might be attributed to both the quantum size effect [28] and electronic properties of zeolite framework [29]. The interaction of iridium nanoparticles with the framework oxygen of the zeolite framework is expected to induce a positive charge on the surface metal, which would increase the binding energies of iridium(0) nanoparticles and has already been observed for the zeolite framework stabilized Ru [13,15], Co [30], and Pt [31] nanoparticles.

The changes in the micropore volume and area of the host material zeolite-Y upon the formation of iridium(0) nanoparticles were investigated by the nitrogen-adsorption-desorption technique (N_2-Ads. Des.). N_2-Ads.-Des. isotherms of zeolite-Y and IrNPs@FAU are given in Fig. 4, and both of them show type I shape, a characteristic of microporous materials [32]. We found that the micropore area (from 753 to 680 m^2/g) and volume (from 0.333 to 0.290 cm^3/g) are reduced on passing from zeolite-Y to IrNPs@FAU, which can be attributed to the formation of iridium(0) nanoclusters within the cavities of zeolite-Y as well as iridium(0) nanoparticles on the external surface.

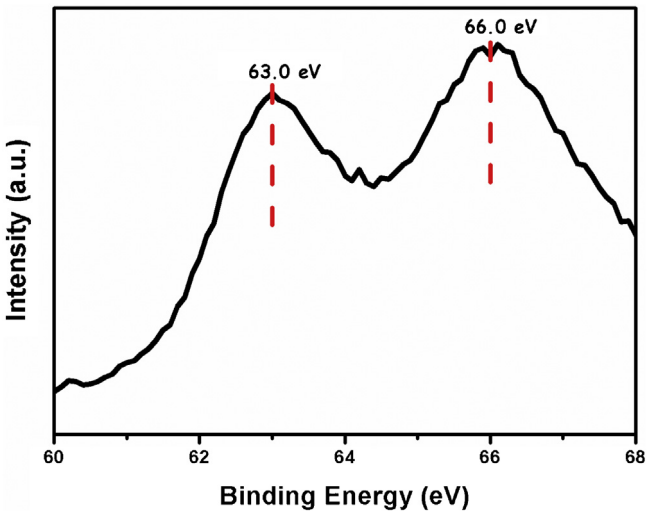

Fig. 3. High resolution Ir 4f XPS spectrum of IrNPs@FAU with an iridium loading of 0.34 wt %.

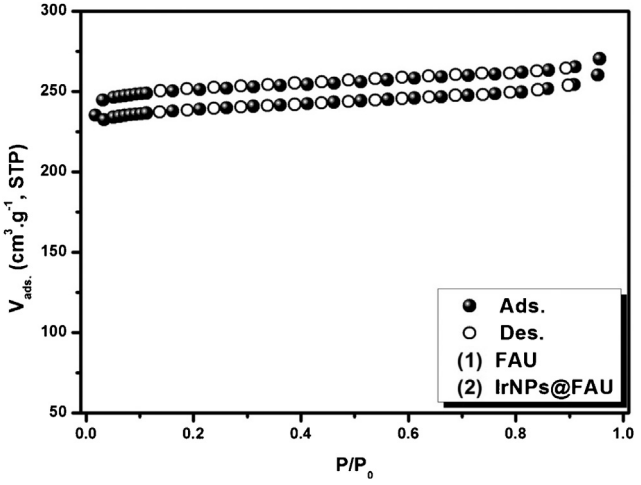

Fig. 4. N_2-adsorption-desorption isotherms of zeolite-Y and IrNPs@FAU with an iridium loading of 0.34 wt %.

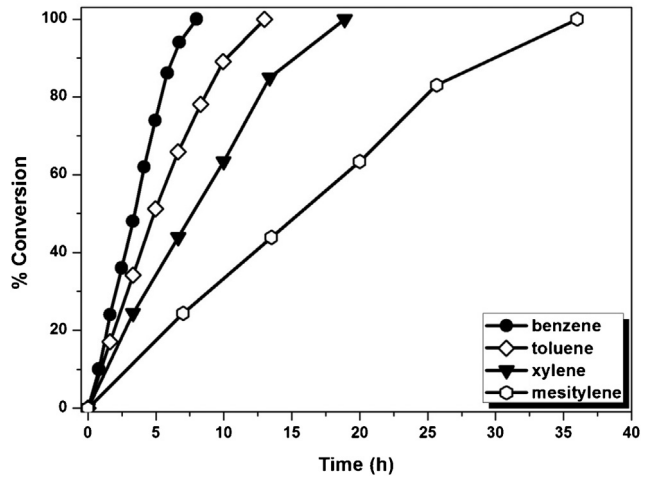

Fig. 5. % Conversion versus time (h) graph for the IrNPs@FAU (87 mg with an iridium loading of 0.34% wt corresponds to 1.54 μmol) catalyzed hydrogenation of • benzene (1.0 mL; 11.22 M), □ toluene (1.0 mL, 9.44 M), ► *o*-xylene (1.0 mL, 8.28 M), ◊ mesitylene (1.0 mL, 7.18 M) at 298 K and 3 bar initial H_2 pressure under solvent-free conditions.

3.2. Catalytic activity of iridium(0) nanoparticles dispersed in zeolite matrix in hydrogenation of aromatics under mild conditions

The catalytic activity of IrNPs@FAU was tested in the hydrogenation of aromatics (benzene, toluene, *o*-xylene, and mesitylene) in the solvent-free systems under mild conditions. The catalytic hydrogenation of aromatics was performed starting with IrNPs@FAU (0.34 wt.% Ir), dispersed in the liquid aromatic by agitating, at 298 K and 3 bar initial H_2 pressure and the progress of the reaction was followed by monitoring the hydrogen uptake which can be converted to the concentration loss of the aromatic substrate by using the stoichiometry. The complete hydrogenation of aromatics was also confirmed by checking the ^{1}H NMR spectra of the reaction solution at the end of the reaction. Before testing the catalytic activity of IrNPs@FAU in the hydrogenation of aromatics, we investigated the effect of iridium loading (% wt) on the activity of IrNPs@FAU. Catalytic activity tests were performed starting with IrNPs@FAU samples all containing 1.54 μmol Ir but in different iridium loading of zeolite (0.34, 0.92, 1.76 and 2.42 wt%) in the hydrogenation of neat benzene at room temperature. The *initial* hydrogen uptake rates were found to be 4.3, 4.0, 3.96 and 3.8 psi H_2/min for the IrNPs@FAU samples containing 0.34, 0.92, 1.76 and 2.42% wt Ir, respectively. The variation in the *initial* hydrogen uptake rates reflects the accessibility of iridium(0) nanoparticles in the zeolite framework by the substrate. The highest catalytic activity is obtained by using IrNPs@FAU sample containing 0.34 wt% Ir, mostly on the surface and readily accessible. The small size of IrNPs@FAU containing 0.34 wt% Ir may be another reason for its high activity. Although, informative TEM images of the 0.92, 1.76 and 2.42 wt% Ir samples could not be obtained, these samples are expected to have larger iridium(0) nanoparticles than the sample containing 0.34 wt% Ir. For all the other test reactions performed in this study, samples of IrNPs@FAU containing 0.34 wt% Ir were used.

Fig. 5 shows the plots of concentration loss of aromatics vs time for the hydrogenation of neat aromatics (benzene, toluene, *o*-xylene, and mesitylene) catalyzed by IrNPs@FAU. For all of the substrates the hydrogenation starts immediately without an induction period as a preformed catalyst is used. A linear hydrogenation continues until the consumption of benzene, toluene, *o*-xylene, and mesitylene with *initial* TOF values [33] of 3190, 1907, 1180, and 490 h^{-1}, respectively. The observed trend in the hydrogenation rate of these substrates (benzene > toluene > *o*-xylene > mesitylene) can be explained by the increasing number of methyl substituents, because of the electronic effect on the aromatic ring due to the addition of methyl groups [34,35]. Additionally, the observation of the slowest hydrogenation rate for mesitylene can also be explained by the Lennard–Jones kinetic diameter of mesitylene (7.6 Å) [36] which is larger than the supercage aperture of zeolite-Y (7.4 Å) [36]. Mesitylene cannot go into the cages of zeolite and, therefore, can be activated only by the iridium(0) nanoparticles on the external surface of zeolite. The iridium(0) nanoclusters in the cages of zeolite-Y are not accessible for the large mesitylene. The TOF value (3190 h^{-1}) obtained for the complete hydrogenation of neat benzene, a well-known test reaction in arene hydrogenation, is lower than that of the previously reported best catalyst (Ru–Ni/C; TOF = 7905 h^{-1}) [19] but higher than the majority of the other catalysts used in the hydrogenation of benzene under mild conditions (Table 1).

More importantly, notable activity difference in the benzene hydrogenation is observed between our new catalyst system and our previous zeolite supported Ir NPs catalyst (TOF = 47 h^{-1}) [17] in which we used $[Ir(COD)Cl]_2$@zeolite as a precatalyst and generated zeolite supported iridum(0) nanoparticles under *in situ* conditions during the hydrogenation of benzene. In that study, we found that the majority of the resulting iridium(0) nanoparticles exist on the surface of the zeolite in agglomerated clump form, resulting from the solution phase impregnation instead of ion-exchange which was impossible with $[Ir(COD)Cl]_2$ precursor. Expectedly, their sizes are larger than that of IrNPs@FAU. Additionally, these iridium(0) nanoparticles were formed from the *in situ* H_2 reduction of surface weakly bound $[Ir(COD)Cl]_2$ and because of that the system contains chloride in 1/1 (Ir/Cl) molar ratio, which can interact with the surface iridium atoms in iridium(0) nanoparticles and decrease their accessibility by the substrate molecules.

The high catalytic activity of IrNPs@FAU can be explained by considering several important factors. First of all, as emphasized in the introduction, iridium was employed as catalyst in hydrogenation of benzene because it is one of the three metals providing the low activation barrier for the dissociation of H_2 favored by strong H-surface interaction and further reaction with the adsorbed —CH=CH— group [37,38], which is also known as "Sabatier Principle" and can be applied to a range of catalytic transformations [39]. The accessibility of surface hydrogen is an important criterion for the further reaction of substrate. In the case of bulk iridium metal, hydrides formed from the dissociation of H_2 can diffuse so deep into the bulk that they are not accessible for the substrate (benzene)

molecule. However, for the iridium nanoparticles the diffusion length is limited by the particle size, and therefore surface hydrogen can easily be accessed by the substrate (benzene) molecules [40]. Furthermore, in our catalyst system, iridium(0) nanoparticles are not covered by ligands, polymers or anionic groups, which would hinder the accessibility of surface iridium atoms for the substrate molecules [41]. The nanoparticles do interact with support only on one side; therefore, they can be considered as half-naked or open to the substrate molecules. Since iridium(0) nanoparticles are small they have large fraction of catalytically active atoms on the surface. Consequently our catalyst shows very high catalytic activity in hydrogenation of neat benzene to cyclohexane.

3.3. Catalytic lifetime of iridium(0) nanoparticles dispersed in zeolite matrix (IrNPs@FAU) in the hydrogenation of neat benzene under mild conditions

The catalytic lifetime of IrNPs@FAU in the hydrogenation of neat benzene was determined by measuring the total turnover number (TTO) at 298 K and 3 bar initial H_2 pressure. When all of the benzene was converted to cyclohexane, more benzene was added into the solution and the reaction was continued in this way until no hydrogen uptake was observed. We found that IrNPs@FAU provide 197000 total turnovers in the hydrogenation of neat benzene over 105 h before deactivation. The apparent *average* TOF value of that corresponds to 1880 h^{-1} which is approximately 60% of the *initial* TOF value of 3190 h^{-1} and indicative of the deactivation of Ir NPs as the catalytic reaction proceeds. Nevertheless, this is the longest catalytic lifetime reported to date since the highest TTO known for neat benzene hydrogenation is 177,200 [15].

3.4. Reusability performance of iridium(0) nanoparticles dispersed in zeolite matrix (IrNPs@FAU) in the hydrogenation of neat benzene under mild conditions

After the complete hydrogenation of neat benzene in a standard experiment, IrNPs@FAU were isolated as powders by suction filtration and dried under vacuum at room temperature. The IrNPs@FAU sample can be safely bottled and stored under ambient conditions. Fig. 6(a) shows the variation in the *initial* TOF values of IrNPs@FAU determined for the catalytic reuse experiments in the hydrogenation of neat benzene. As seen from Fig. 6(a), when reused, IrNPs@FAU catalyst retains > 50% of its *initial* catalytic activity after five cycles (*initial* TOF = 1800 h^{-1} at 5th reuse) achieving the complete hydrogenation of benzene in each cycle without jeopardizing the selectivity. The decrease in the catalytic activity of IrNPs@FAU can be attributed to a decrease in the number of active surface atoms of iridium(0) nanoparticles from 5.8 ± 2.1 nm to 8.1 ± 2.9 nm as measured for IrNPs@FAU sample harvested from the fifth catalytic run (Fig. 6(b)).

Importantly, no iridium leaching was detected in the filtrate solution collected at the end of the reaction (analyzed by ICP-MS with a detection limit of 35 ppb for Ir). A control experiment showed that the hydrogenation of benzene did not continue after IrNPs@FAU was removed shortly after the reaction had started, confirming no leaching of active catalyst to the solution.

3.5. Tricyclohexylphoshpine ($P(C_6H_{11})_3$) poisoning of iridium(0) nanoparticles dispersed in zeolite matrix (IrNPs@FAU) in the hydrogenation of benzene

Although TEM images show unequivocally the presence of iridium(0) nanoparticles on the external surface of zeolite-Y, the N_2-Ads.-Des. isotherms and the sharp decrease in the hydrogenation rate of mesitylene compared to that of other aromatics imply the existence of iridium(0) catalyst within the cages of zeolite-Y as

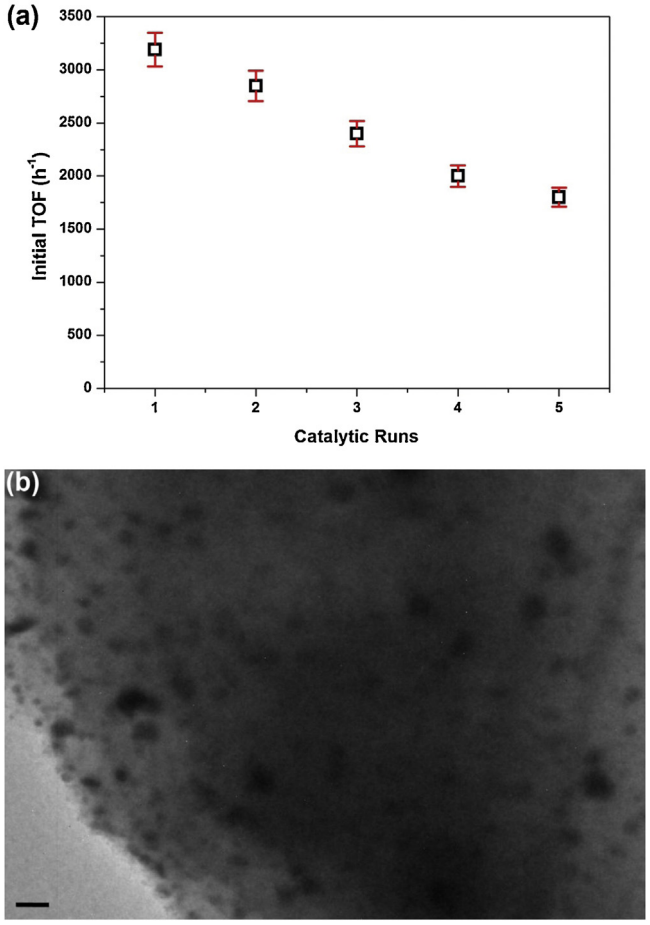

Fig. 6. (a) Plot initial TOF values (h^{-1}) versus number of catalytic runs for the reusability of IrNPs@FAU in the hydrogenation of neat benzene (1.0 mL; 11.22 M); (b) TEM image of the IrNPs@FAU sample harvested from the 5th catalytic reuse in the hydrogenation of neat benzene (scale bars represents 5 nm).

well, which are not accessible by large molecules such as mesitylene. In order to check the distribution of catalytically active sites on the external surface and/or in the cages of zeolite-Y, we performed poisoning experiments by using tricyclohexylphosphine ($P(C_6H_{11})_3$) which has kinetic diameter of 10.9 Å [42] and cannot enter the supercages through the 7.4 Å aperture of zeolite. Therefore, $P(C_6H_{11})_3$ ligand can only poison the iridium(0) nanoparticles supported on the external surface of zeolite-Y, but can not poison the iridium(0) nanoparticles in the cavities of zeolite-Y.

For that purpose, the hydrogenation of neat benzene catalyzed by IrNPs@FAU was conducted in the presence of $P(C_6H_{11})_3$ ligand in various $P(C_6H_{11})_3$/Ir molar ratios at 298 K. The initial rate of benzene hydrogenation was determined in each of the independent experiments at various $P(C_6H_{11})_3$/Ir ratios (0.05, 0.10, 0.15, 0.20 and 0.25) and divided by the hydrogenation rate of neat benzene in the absence of $P(C_6H_{11})_3$ at 298 K to obtain the catalytic activity retained. Fig. 7 shows the plots of the percent catalytic activity retained in the hydrogenation of neat benzene versus $P(C_6H_{11})_3$/Ir molar ratio. In the hydrogenation experiments performed in the presence of $P(C_6H_{11})_3$, the catalytic activity of IrNPs@FAU decreases almost linearly with the increasing concentration up to $P(C_6H_{11})_3$/Ir = 0.15 and further addition of $P(C_6H_{11})_3$ ($P(C_6H_{11})_3$/Ir = 0.20 and 0.25) did not effect the catalytic activity of IrNPs@FAU. First of all, the suppression of catalytic activity by phosphine ligand addition into IrNPs@FAU catalyzed benzene hydrogenation is compelling evidence for a heterogeneous catalysis [43]. Secondly, Fig. 6 indicates that the IrNPs@FAU has 45% of the

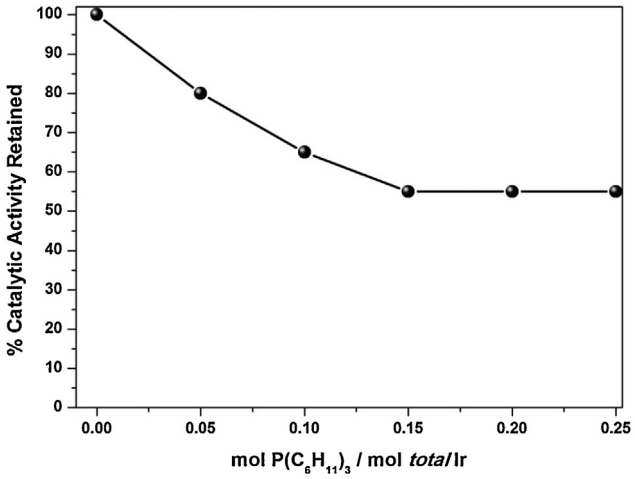

Fig. 7. Plot of % catalytic activity of IrNPs@FAU retained versus mol poison/total mol Ir ratio for the $P(C_6H_{11})_3$ poisoning in the hydrogenation of 1.0 mL of neat benzene catalyzed by IrNPs@FAU (87 mg with an iridium loading of 0.34% wt corresponds to 1.54 μmol) at 298 K and 3 bar initial H_2 pressure.

catalytically active Ir NPs standing on the external surface of the zeolite, while the remaining 55% are in the cavities of the zeolite-Y, as the large phoshine $P(C_6H_{11})_3$ ligand can not enter the zeolite cages and the iridium(0) clusters within the zeolite cages are not poisoned by $P(C_6H_{11})_3$ and remain catalytically active even after addition of poison.

4. Conclusions

IrNPs@FAU have been reproducibly prepared from the borohydride reduction of Ir^{3+}@FAU and characterized by several advanced analytical tools. They have been employed as catalytic material in the hydrogenation of aromatic substrates in solvent-free systems under mild reaction conditions (298 K and 3 bars of initial H_2 pressure). This material demonstrates exceptional catalytic lifetime (TTON = 197,000) with remarkably high catalytic activity (TOF = 3190 h^{-1}) and reusability (>50% of inherent activity after the fifth reuse at 100% conversion) in the complete hydrogenation of neat benzene. Moreover, IrNPs@FAU catalyzed solvent-free hydrogenation of aromatics is "relatively green" in terms of its environmental impact as it fulfils the majority of the green chemistry requirements [33] including the followings: (i) it is 100% selective and minimizes by products or waste; (ii) it maximizes the incorporation of all reactants into the products; (iii) it is solventless (i.e., uses neat aromatics as the substrate/solvent); (iv) it requires relatively low energy as it occurs under mild conditions of 298 K and 3 bar of H_2 pressure; (v) it is catalytic, not stoichiometric; (vi) it does not use any blocking, protecting/deprotecting group; (vii) real-time monitoring is easy by measuring the H_2 uptake, ^1H NMR, or GC analysis, for example.

Acknowledgment

Partial support by Turkish Academy of Sciences is acknowledged.

References

[1] M. Hudlicky, Reductions in Organic Chemistry, ACS, USA, 1996.
[2] R.C. Larock, Comprehensive Organic Transformations, Wiley-VCH, New-York, 1999.
[3] J.H. Gary, G.E. Handwerk, Petroleum Refining Technology and Economics, Marcel Dekker, Germany, 1984.
[4] J. Ende, Chemical Engineering in the Pharmaceutical Industry, Wiley-VCH, New-Jersey, 2011.
[5] A Webofscience literature search for the terms "benzene hydrogenation" and "catalyst" hits 1762 references where 95% of them are related to catalytic transformation.
[6] T.W.G. Graham, C.B. Frhyle, Organic Chemistry, Wiley-VCH, New-Jersey, 2011.
[7] M.H. Seeberger, R.A. Jones, J. Chem. Soc. Chem. Comm. 6 (1985) 373.
[8] Z. Duan, A.P. Sylwester, M.J. Hampden-Smith, Chem. Mater. 4 (1992) 1146.
[9] H.H. Hwu, J. Eng, J.G. Chen, J. Am. Chem. Soc. 124 (2002) 702.
[10] J.P. Nicholas, H. Ahn, T.J. Marks, J. Am. Chem. Soc. 125 (2003) 4325.
[11] V. Mevellec, E. Ramirez, K. Phillippot, B. Chaudret, A. Roucoux, Adv. Synth. Catal. 346 (2004) 72.
[12] J. Zhang, Z. Xie, Z. Liu, W. Wu, B. Han, J. Huang, T. Jiang, Catal. Lett. 103 (2005) 59.
[13] M. Zahmakiran, S. Ozkar, Langmuir 24 (2008) 7065.
[14] H.B. Pan, C.M. Wai, J. Phys. Chem. C 113 (2009) 19782.
[15] M. Zahmakiran, Y. Tonbul, S. Ozkar, J. Am. Chem. Soc. 132 (2010) 6541.
[16] M. Zahmakiran, Y. Tonbul, S. Ozkar, Chem. Commun. 46 (2010) 4788.
[17] E. Bayram, M. Zahmakiran, S. Ozkar, R.G. Finke, Langmuir 46 (2010) 12455.
[18] M. Zahmakiran, Y. Roman-Leshkov, Y. Zang, Langmuir 28 (2012) 60.
[19] L. Zhu, L. Zheng, K. Du, H. Fu, Y. Li, G. You, B.H. Chen, RSC Adv. 3 (2013) 713.
[20] F. Li, B.C. Gates, J. Phys. Chem. C 111 (2007) 262.
[21] M. Zahmakiran, S. Özkar, Langmuir 25 (2009) 2667.
[22] M. Zahmakiran, S. Akbayrak, S. Özkar, Dalton Trans. 39 (2010) 7521.
[23] M. Poliakoff, J.M. Fitzpatrick, T.R. Farren, P.T. Anastas, Science 297 (2002) 807.
[24] S. Özkar, L. McMurray, A. J. Holmes, A. Kuperman, G.A. Ozin, J. Phys. Chem. 95 (1991) 9448.
[25] R. Jelinek, S. Özkar, G.A. Ozin, J. Am. Chem. Soc. 114 (1992) 4907.
[26] W. Chen, S. Chen, J. Mater. Chem. 21 (2011) 9169.
[27] C. Wagner, W.M. Riggs, L.E. Davis, J.F. Moulder, G.E. Muilenberg, Handbook of X-ray Photoelectron Spectroscopy, in: Physical Electronic Division, Perkin-Elmer, Eden Prairie, MN, 1979, pp. 55.
[28] G. Schmid, Clusters Colloids; From Theory to Applications, VCH Publishers, New York, 1994.
[29] Y.-X. Jiang, W.-Z. Weng, D. Si, S.-G. Sun, J. Phys. Chem. B 109 (2005) 7637.
[30] L. Guczi, D. Bazin, Appl. Catal. A 88 (1999) 163.
[31] A. Fukuoko, N. Higashimoto, Y. Sakamoto, S. Inagaki, Y. Fukushima, M. Ichikawa, Top. Catal. 18 (2002) 73.
[32] S. Storck, H. Bretinger, W.F. Maier, Appl. Catal. A 174 (1998) 137.
[33] The TOF and TTO values reported herein are those typically reported. TOF = mol of H_2 consumed/total mol of catalyst loading)/time; TTO = TOF time. That is, the reported values of TOF and TTO are not corrected for the amount of metal that is on the surface of the catalyst and/or the actual number of active sites. For the calculation of initial TOF values ~ 40% conversions of substrates were considered.
[34] G.S. Fonseca, E.T. Silveira, M.A. Gelesky, J. Dupont, Adv. Synth. Catal. 347 (2005) 847.
[35] M.V. Bahaman, M.A. Vannice, J. Catal. 251 (1991) 251.
[36] D.W. Breck, Zeolite Molecular Sieves, Krieger, Malabal, FL, 1984.
[37] J.A.M. Simoes, J.L. Beauchamp, Chem. Rev. 90 (1990) 629.
[38] J. Greeley, J.K. Norskov, M. Mavrikakis, Annu. Rev. Phys. Chem. 53 (2002) 319.
[39] P. Sabatier, La Catalyse en Chimie Organique, Breange, Paris, 1920.
[40] A.M. Doyle, S.K. Shaikhutdinov, S. David Jackson, H.-J. Freund, Angew. Chem. Int. Ed. 42 (2003) 5240.
[41] M. Zahmakiran, S. Ozkar, Nanoscale 3 (2011) 3462.
[42] X. Li, G.A. Ozin, S. Ozkar, J. Phys. Chem. 95 (1991) 4463.
[43] B.J. Hornstein, J.D. Aiken, R.G. Finke, Inorg. Chem. 41 (2002) 1625.